

# Competition of van der Waals and chemical forces on gold–sulfur surfaces and nanoparticles

**Reimers, Jeffrey R.; Ford, Michael J.; Marcuccio, Sebastian M.; Ulstrup, Jens; Hush, Noel S.**

*Published in:*
Nature Reviews. Chemistry

*Link to article, DOI:*
10.1038/s41570-0017

*Publication date:*
2017

*Document Version*
Peer reviewed version

**REVIEW ARTICLE:**

# Competition of van der Waals and chemical forces on gold-sulfur surfaces and nanoparticles

*Jeffrey R. Reimers[1,2], Michael J. Ford[2], Sebastian M. Marcuccio[3,4], Jens Ulstrup[5], and Noel S. Hush[6,7]*

[1] International Centre for Quantum and Molecular Structures, College of Sciences, Shanghai University, Shanghai 200444, China.

[2] School of Mathematical and Physical Sciences, The University of Technology Sydney, Sydney NSW 2007 Australia.

[3] Department of Chemistry and Physics, La Trobe Institute for Molecular Science, La Trobe University, Melbourne, Victoria 3086, Australia.

[4] Advanced Molecular Technologies Pty Ltd, Unit 1, 7-11 Rocco Drive Scoresby, Vic. 3179, Australia.

[5] Department of Chemistry, Technical University of Denmark, Kongens Lyngby 2800, Denmark.

[6] School of Chemistry F11, The University of Sydney, NSW 2006 Australia.

[7] School of Molecular Bioscience, The University of Sydney, NSW 2006 Australia.

## TOC graphic

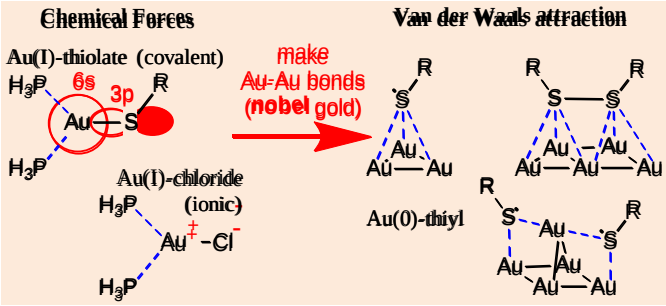



## Abstract

Chemists generally believe that covalent and ionic bonds form much stronger links between atoms than does the van der Waals force. However, this is not always so. We present cases in which van der Waals dispersive forces introduce new competitive bonding possibilities rather than just act to modulate traditional bonding scenarios. Although the new possibilities could arise from any soft-soft chemical interaction, we focus on bonding between Au atoms and alkyl/arylsulfur ligands RS. The structural, chemical, and spectroscopic properties of sulfur-protected gold surfaces and gold nanoparticles can only be understood in this light, whence pathways to new chemical entities and innovative nanotechnological devices are opened. A broad overview is given of modern computational methods appropriate to six fields ranging from gas-phase chemistry to biochemistry to device physics.


Covalent and ionic bonds are usually described as providing strong chemical forces demanding specific bond lengths, with covalent bonds also demanding an inner coordination sphere with well-defined molecular structure. On the other hand, the non-covalent van der Waals dispersion force is thought to bring molecules together in less directional ways. The force generates weak individual interatomic attractions that occur over widely ranging interaction distances and topologies. The importance of the dispersion attraction arises as all of the atoms in interacting molecules contribute to a significant combined effect. Concerning individual atom-atom bonds, what is being recognized now is that there also exists an intermediate regime in which the real or apparent dispersion force is of a magnitude comparable to that of the covalent and ionic forces. Some examples of this are sketched in Figure 1.

The dispersion force is quantum-mechanical in origin and can be described in terms of the effect of dipoles produced by quantum fluctuations on one atom or molecule attractively polarizing its environment.[1] All electrons in interacting bodies contribute to the effect, which becomes large when highly polarizable species are involved. The dispersion force is the dominant interaction occurring between neutral molecules at large separations. However, it remains operative in all chemical scenarios, forming a component of the bond strength that reinforces covalent and/or ionic bonding processes. It is usually not possible to ‘switch off’ the dispersion force, an exception being when two molecules or objects are

separated by a Faraday cage.[1,2] A key feature is that the total dispersion force between two parts of *the same* molecule can become channelled through a single bond (Fig. 1).

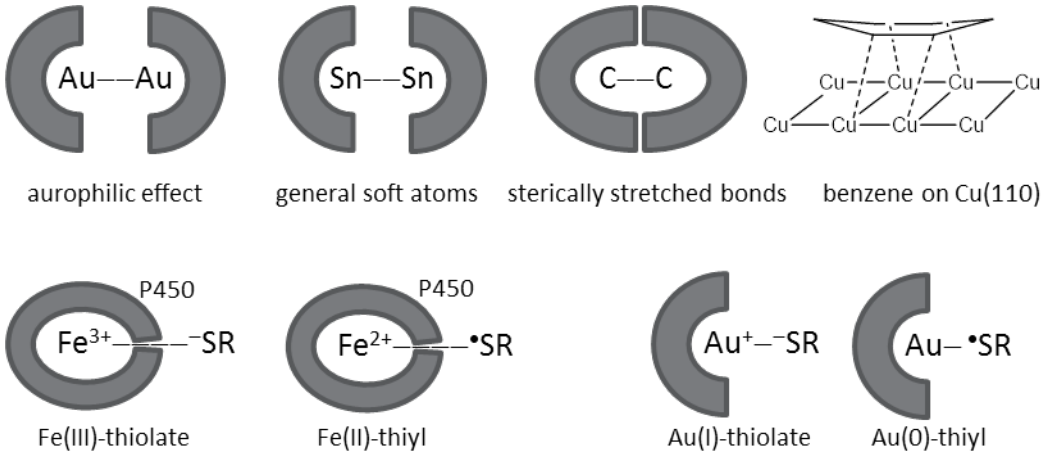


**Figure 1:** Ways that van der Waals dispersion forces can modify chemical bonding. The top row shows examples of how dispersion forces make existing bonds stronger and more stable in unusual geometries, whilst the bottom row shows dispersion forces leading to alternate chemical structures.

For bonds between gold atoms, bond strengths larger than what is easily explicable based on usual notions of ionic and covalent bonding have long been recognised and termed the "aurophilic effect", something now understood in terms of unusually strong dispersion forces of typical strength 5-15 kcal $mol^{-1}$.[3,4] Increasingly, chemists have realised that strong dispersion forces are more pervasive, with much work focusing on molecules containing e.g., Sn-Sn bonds[5] and Ge-Ge or Pb-Pb bonds.[6] Similar effects were seen even with C-C bonds[7-9] and bonds between other main-group elements[10,11] that, because of steric crowding in a molecule, are forced to become far longer than usual. In these compounds, the bond strength decreases less sharply at long lengths than one would expect if only covalent bonding were at play. Significant enhancement to the stability of transition-metal complexes from dispersion forces has also been observed.[12] In some cases, individual atom-atom dispersion forces are large, whilst in others, heavy groups on each side of the bond interact with each other in such a way that the forces are all channelled through the central bond, giving an apparently large atom-atom dispersion interaction.

Independent of mechanism, for all the examples in Fig. 1, the usual chemical bonding effects and the dispersion interaction operate together. Such cooperativity is well known in the field of hydrogen bonding, but in that case the dispersion forces are small enough to be neglected in simple models.[13] The structures presented in Fig. 1 can only be rationalized if dispersion force effects are considered. Of particular current interest is the situation in which strong dispersion forces change the shape of the ground-state potential-energy surface enough to facilitate unexpected chemical processes.[10,14-17] The formation of benzene from acetylene on Cu(110) is facilitated in this way,[18,19] and the adsorption of benzene on coinage metals provides benchmarks for the quality of computational methods in treating dispersion interactions involved in self-assembly.[20] The interaction of adsorbed benzene with Cu(110) is

dominated by van der Waals interactions, whose collective strength is comparable to that of typical covalent bonds.[19] We will return below to the question of how to perform calculations for chemical processes in which dispersion forces play significant roles.

**Different chemical forms of the same species**

Described in Figure 1 are two situations in which the interplay between covalent and van der Waals forces manifests two different chemical forms of the one species. One example involves valence tautomerisation depicting equilibrium between isomers, the other resonance stabilization depicting the mixing of different bonding forms into the one structure.

The valence tautomerization example considers the bond between the iron of the heme group in cytochrome P450 and an attached cystyl ligand.[21] Simple heme groups ligated by SR compounds form model systems for this biochemical process. Observed are two structurally distinct forms of the Fe-S bond

$$\underset{\text{ferrous thiyl}}{\text{Fe(II)} - {}^{\bullet}\text{SR}} \underset{\longleftarrow}{\overset{\text{H}_2\text{O etc.}}{\longrightarrow}} \underset{\text{ferric thiolate}}{\text{Fe(III)} - {}^{-}\text{SR}} .$$

The evidence supporting this analysis is summarized in Box 1.[21] Related aspects of tautomerism apply also to the iron/heme/oxygen ligand interactions in the heme peroxidases and catalases.[22] Valence tautomerisation is like any isomerization reaction and is equivalent, for example, to the pyramidal inversion that interchanges the orientation of the molecular dipole in ammonia.[23] The critical feature of the P450 model compounds[21] is that one valence tautomer is stabilized by a covalent bond whilst the other is stabilized only by the dispersion interaction.

**Box 1 | Observations indicating valence tautomerization in P450 model compounds**

- Two isomeric structures are observed in equilibrium at room temperature.
- These have distinct resonance Raman frequencies for the Fe-S stretch, as well as for modes related to the macrocyclic ring and substituent R.
- Electron paramagnetic resonance indicates that one species is Fe(III) whilst the other is Fe(II), with associated change in the S signal also apparent.
- There is also a large change in the nuclear magnetic resonance signal.

Before considering the second example, we discuss basic aspects of resonance stabilization and compare these to valence tautomerisation. The classic example of resonance stabilization is benzene, whose ground state at room temperature exists as a single isomer featuring six equal C-C bond lengths. Alternatively, benzene could have existed as an equilibrium mixture of its two tautomeric Kekulé structures, each representing one of the two possible forms with alternating single and double bonds. These two classic chemical structures interact with each other through resonance. Resonance is a universal property and also acts to mix the valence tautomers found in the previously discussed cytochrome P450 model compounds. In the case of P450 the resonance energy is small and model compounds can be found in different tautomers containing distinctly different character. However, in benzene the resonance energy is large, such that only a single ground-state structure exists,

with properties that are the average of the individual Kekulé structures. Resonance is also always important in determining excited-state spectroscopic properties. When valence tautomers are not symmetrically equivalent, dispersion forces affect each tautomer individually. This can change the identity of the lowest-energy tautomer, indirectly determining key chemical and spectroscopic properties. Incorporating all of these features, a general theory for chemical structure, reactivity, and spectroscopy can be constructed to quantify the far-reaching effects of resonance, smoothly linking valence tautomerisation to aromaticity.[24] Profound results have followed, including: finding the factor that differentiates between the dominance of tetrahedral bonding patterns for first-row elements and seemingly octahedral ones for later rows,[23] determining what chemical reactions may be useful as hosts for qubits in quantum information processors,[25,26] and understanding the fundamental nature of breakdown of the Born-Oppenheimer approximation in chemistry.[27] Importantly, valence tautomerisation and resonance stabilization are just two extremes of the same phenomenon, and real systems always contain mixtures of both types of characteristics.

The second example considered in Fig. 1 highlights the role of dispersion in a resonance-dominated scenario. An understanding of this system requires an appreciation of the bonding between gold and sulfur ligands SR in molecular compounds, thin films, nanoparticle coverings, and surface monolayers.[28] Two alternate chemical structures are in resonance with each other:

$$\underset{\text{gold thiyl}}{\text{Au(0)} - {}^{\bullet}\text{SR}} \longleftrightarrow \underset{\text{gold thiolate}}{\text{Au(I)} - {}^{-}\text{SR}}$$

These resonance structures are not in thermal equilibrium, but rather a single hybrid ground-state isomer can only be found. Key results[29-45] leading to this conclusion are summarized in Box 2. As the relative energies of the two resonance structures changes with environment, the ground-state bonds can be made to vary smoothly in character between the two limiting forms. Always there exists an excited state with properties alternate to that of the ground state, e.g., if the ground state is largely Au(0)-thiyl then there will exist an excited state that is largely Au(I)-thiolate.[24] The interpretation of observed properties of Au-S bonds is further complicated because Au(I)-thiolates can themselves exist as resonance hybrids of two canonical forms in which the gold is represented as either $d^{10}s^0$ (the lower energy form) or $d^9s^1$ (the higher energy form). Changing Au hybridization mixes these forms. Modern electronic structure calculations reveal signatures of Au(0)-thiyl bonding, as well as for both the $d^{10}s^0$ and $d^9s^1$ types of Au(I)-thiolate bonding, in all types of Au-S bonds. Sometimes observables like chemical reactivity and allowed/forbidden transitions are determined by the *dominant* character present in each situation, whereas other properties access only the *small amount* of alternate character that is mixed in. As Box 2 shows, the dominant character of Au-S bonds change from $d^{10}s^0$-dominated Au(I)-thiolate bonding in compounds and thin films to largely Au(0)-thiyl bonding in large nanoparticles and on Au(111) surfaces.[28]

**Box 2 | Observations indicating Au(0)-thiyl dominates surface and nanoparticle interfaces**

- In a wide range of chemical environments involving Au-SR bonds, X-ray photoelectron spectroscopy of the Au 4*f* level indicates[29-34] binding energies of 83.8-84.5 eV, typical of Au(0). For reference, the binding energies of Au(I) compounds are much larger, being 85.5-85.8 eV for oxides[35-37] and sulfides,[38] with values in the vicinity of 84.9 eV reported for Au(I)-thiolate compounds.[29,39,40] Bracketing these, Au(III) complexes absorb near 86.5 eV, while anionic gold absorptions have been reported down to 82.6 eV.[41,42]
- X-ray absorption near-edge spectroscopy of nanoparticle surfaces reveals the contributions of Au(I)-thiolate resonance structures mixed with Au(0)-thiyl. Qualitatively, the data implicate Au $d^9s^1$ as the most important term and quantify its contribution as 7% for nanoparticles of 4.0 nm diameter, increasing to 11% as the diameter decreases to 1.6 nm.[43] These results are consistent with the intensities of weak tails seen in high-resolution Au 4*f* photoelectron spectroscopy at ~85 eV.[34,43]
- A wide range of experimental and computational data indicate that Au-S bonds exhibit weak charge polarization ($Au^{\delta+}$-$S^{\delta-}$), such that some ionic Au(I)-thiolate bonding character is always present, independent of the chemical environment.[28] However, for SR monolayers on Au(111), the surface dipole moment is oriented such that the *surface* has a net *negative* charge and the ligands a net positive charge.[44] This indicates that Au(I)-thiolate structures are only minor contributors to the ground-state resonance hybrid, the most significant electrostatic effect being the flow of electron density from the dominant electropositive atoms present, H atoms in the R group, to the dominant electronegative atoms present, Au.
- Near-edge X-ray absorption fine structure (NEXAFS) measurements of RS species bound to surfaces have been interpreted using density functional theory (DFT) calculations, which reveal the destination orbital involved in the transition to be mostly of S character, with some admixed Au *d* component.[45] The Au *d* orbitals' participation in bonding indicates that the dominant form of any Au(I)-thiolate species involved must have the Au $d^9s^1$ configuration. In this configuration, the destination orbital would by definition already be doubly occupied in a pure Au(I)-thiolate species. Hence the Au(I)-thiolate description is inappropriate as it regards the *observed* transition as being formally *forbidden*. The observed spectrum is only consistent with an Au(0)-thiyl bonding description, into which a small amount of Au(I)-thiolate character is mixed by resonance.[28]
- Basic chemical properties of molecular compounds and thin films follow qualitative trends for Au(I)-thiolate bonding. Alternatively, only Au(0)-thiyl bonding can explain the properties of large nanoparticles and surfaces, predicting smooth variations as surface-bound RS and RSSR or sulfides and polysulfides interconvert. Similar smooth changes are at play when the S linking atoms are substituted with C, N, P, O, Se, or Te linkers.

As an example of how this description encompasses all known properties of Au-S bonds, we consider briefly the interpretation Au 4*f* XPS spectra. These spectra reveal variations indicative of the chemical bonding environment of gold atoms at or near gold surfaces and nanoparticle surfaces. Observed bands vary by over 4 eV in terms of the band-centre position, revealing the binding energy of the 4*f* electrons[29-36,38-42] to provide characteristic descriptors of gold atoms in their -I, 0, I, and III, valence states. Typically broad bands up to 1 eV in width are found in nanoparticles,[32,37,43,46] with sharper bands found on metal surfaces.[30] Band broads are indicative of the presence of atoms in similar chemical environments taking on a range of nuclear structures. In Au(I)-thiolate compounds, the band centre is located in the Au(I) region of 84.9 – 85.8 eV, but on gold nanoparticles and surfaces a broad band in the 83.8 – 84.5 eV range is found. All of this band arises from atoms of primary Au(0) character, but through resonance differing amounts of Au(I) gets mixed in as a function of the nuclear structure, resulting in band broadening. Historically the 83-8-84.5 eV

band has been deconvoluted into the minimum-feasible number of just two components, sometimes labelled "Au(0)" and "Au(I)" as if something akin to valence tautomerisation is being observed,[47] but in reality all that is happening is that the part of the observed band attributed to "Au(I)" comes from gold atoms with just 5-20% Au(I) character.[43,48] Even molecular compounds and thin films properly labelled as "Au(I)-thiolates" may only have 75% Au(I) character, making these species only indicative of what a "pure" Au(I)-thiolate would be.

Covered in this Review are the implications that a Au(0)-thiyl or Au(I)-thiolate description have on chemical reaction mechanisms and nanoparticle syntheses. Rationalizing observables often involves recognizing that reactions can be initiated not only on the ground-state surface but also on the associated excited-state surface. The ground-state is primarily Au(0)-thiyl in character on surfaces and nanoparticles whilst the excited-state is primarily Au(I)-thiolate. However, in molecular compounds the order is reversed, and so the conversion of molecular precursors to nanoparticle products involves a steady change from one chemical form to the other. Understanding this reaction requires these issues to be appreciated from both qualitative and quantitative perspectives.[28] We thus consider how it is that dispersive forces dominating bonding in Au(0)-thiyl species can influence outcomes by competing with covalent and ionic forces in Au(I)-thiolates. A simple bonding picture is developed describing just what the "Au(I)-thiolate" description embodies, with key qualitative indicators identified to allow predictions to be made regarding bonding character. Lastly, a brief overview is given on how quantitative calculations can be made to encompass van der Waals interactions at play in Au-S system of relevant to applications in biochemistry, chemistry, physics, and materials science.

**Hard and soft acids and bases**

Situations in which dispersion forces can start to govern basic chemical properties are most succinctly described in terms of Pearson's theory of hard/soft acids and bases (HSAB),[49-51] depicted in Box 3. Many aspects of chemistry can be explained at a simple level using this approach,[52] which is useful in rationalizing which pairs of Lewis acids and bases are likely to form stable adducts. The issues addressed usually do not consider traditional covalent bonding between many first-row elements but instead focus on more ionic bonding. Indeed, traditional chemical nomenclature for non-first-row compounds is based on the limiting ionic description of the bonding, ignoring any covalency. For example, the complex $[Fe(H_2O)_6]^{2+}$ is described as being Fe(II), even though the actual charge on the iron atom is on the order of +0.8 *e*, owing to the net flow of electrons from O to Fe atoms through covalent bonding.

Box 3 | **Hard and soft acids and bases, covalent, van der Waals, and ionic bonding**

$$A_H + :B_H + A_S + :B_S \rightarrow A_H{-}B_H + A_S{-}B_S$$

| small, high charge density | large, highly polarizable |
|---|---|
| $A_H$- hard acid, e.g., $H^+$, $Na^+$, $Ca^{2+}$, $Fe^{2+}$ | $A_S$- soft acid, e.g., $Cu^+$, $Au^+$, $Hg^{2+}$, $Fe^{2+}$ |
| $B_H$- hard base, e.g., $F^-$, $OH^-$, $H_2O$, $NH_3$ | $B_S$- soft base, e.g., $RS^-$, RSH, $I^-$, CO |

1. Hard acids prefer to react with hard bases, soft acids prefer to react with soft bases

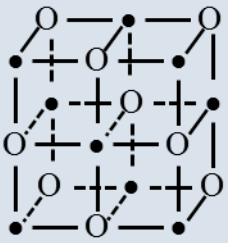

NaCl, 6 bonds per atom

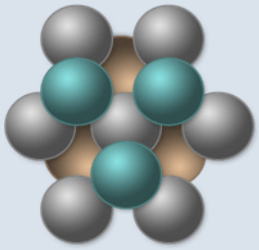

Solid argon, 12 bonds per atom

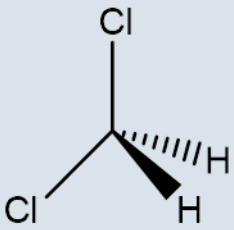


$CH_2Cl_2$ – $sp^3$ bonding

2. Ionic and van der Waals forces allow many angles whilst covalent bonding is prescriptive

In Pearson's definition, hard acids and bases are species that are small and highly charged with large energy-level spacings. Such species interact with each other through strong ionic bonds, exemplified by those in NaCl (Box 3). The ions $Na^+$ and $Cl^-$ are therefore classified as "hard" ions. For NaCl, not only are the atoms in the crystal ionized, but also are those in the diatomic NaCl molecule itself.[53] On the other hand, *soft* acids and bases are large and highly polarizable, and feature small energy-level spacings. These are perceived as interacting strongly with only each other. Highly polarizable species always interact through dispersion forces, though there can also be covalent character to the interaction. Classic "soft" species include Au(I), and, to a lesser extent, Au(III), as well as thiols RSH and thiolates $RS^-$; the "aurophilic" interaction between two Au atoms is a soft-soft interaction.[3,4] The central ansatz of the HSAB model is that hard acids prefer to bind to hard bases whilst soft acids prefer to bind to soft bases (Box 3).

These ideas can be applied to understand some of the unusual features depicted in Fig. 1. If Cu, Ag, and Au as well as benzene were "hard" species then the distances between atoms of these metal surfaces and the adsorbed benzene would follow ionic radii (Cu 0.91 Å, Ag 1.29 Å and Au 1.51 Å). Yet the distances vary only very little, with different computational methods predicting different orders of lengths depending on how dispersion is included.[54] Ionic and covalent bonding would be expected to weaken when moving down the coinage metals, but the adsorption energies are all very similar, perhaps even being greatest in the case of Au.[20,54,55]

An Fe(II) centre can be either hard or soft (Box 3), and it behaves as the latter when bound to hard bases like water in the complex $[Fe(H_2O)_6]^{2+}$. However, in cytochrome P450 and its model compounds, Fe interacts with a soft thiyl/thiolate group and the complex can either stay ferrous to exploit its soft-soft interaction, or undergo valence tautomerisation to the ferric thiolate stabilized by a hard-hard interaction. Hardness decreases and softness

increases down the chalcogens O-S-Se-Te and hence one would expect dispersion forces to grow in importance. Indeed, Au-chalcogen bonds increase in strength down the group,[56] indicating that dispersion forces become dominant over covalent forces as covalent bond strengths decrease down the periodic table owing to reduced orbital overlap.

A weakness of the HSAB approach is that it does not differentiate between covalent and dispersive interactions. Although inorganic complexes are named after their limiting ionic valence form independent of the degree of covalency, covalent effects always govern ligand coordination, as illustrated in Box 3. Ionic bonding can give rise to a multitude of arrangements, including the 6-coordinate NaCl structure. Likewise, van der Waals bonds are non-directional, and give rise to the 12-coordinate structure of solid argon. However, when covalent bonds are involved the coordination becomes highly directional, as it is with the $sp^3$ coordinated C atom of methylene chloride. Neutral sulfur atoms can form at most two covalent bonds, e.g., as in thioethers, thioesters, disulfides and thiols. If sulfur is oxidized or reduced, more bonds can form, and in $SO_4^{2-}$ there are four $S^{2+}$ to $O^-$ covalent bonds such that it has mixed covalent and ionic bonding character[57]

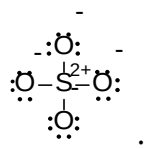

In typical bonding scenarios with gold, sulfur forms three or four bonds, permitted if bonding is either ionic or dispersive in nature but not if sulfur is neutral and bonds only covalently. While Au-S bonds do always have some ionic component, bonding promiscuity increases for Se compounds with Au.[56] However, the ionic character decreases whilst the dispersive character increases, indicating that the dispersive contribution is dominant. The simplest-level description of the bonding in Au-S compounds thus demands inclusion of the dispersion force. This applies regardless of whether a system is classified as Au(I)-thiolate or as Au(0)-thiyl, as the factors controlling coordination and bond angles are not significantly different for the two chemical species. Adding further complication, gold atoms can be considered as a "carbon substitute" as they can form covalent single, double and triple bonds to carbon,[4,58,59] presenting situations for which ionic labels like Au(0) and Au(I) no longer remain useful. One must therefore look beyond simple HSAB descriptions in order to fully understand Au-S chemistry.

**Bonding descriptors for Au interacting with Group-XVI elements**

The valence electronic configuration of gold is $d^{10}s^1$ and so gold can interact with nearby atoms using either *d* or *s* electrons, with relevant chemical bonding scenarios presented in Figure 2. If gold interacts through its *s* orbital then the Au(I)-thiolate scenario results. This figure is drawn so as to exaggerate the energy difference between the gold and sulfur orbitals, as it is the standard practice to name such species based on their limiting ionic form, which results when an infinite energy difference is assumed. In contrast, when S is replaced with Te a Te(II)-auride species forms, with Te being an electropositive metal bound to an electronegative Au atom. The purely covalent scenario, typified by homonuclear

diatomics like $H_2$, occurs when there is no energy difference; this is included in the figure for reference. Despite the change in nomenclature, Au(I)-thiolates and Te(II)-aurides are essentially covalent in nature and have similar properties (though the aurides are more easily oxidized).[60,61] Although the bonding scenarios discussed are extremely well known, an unusual arrangement occurs when the gold *d* orbitals are involved in bonding. In such a case the Au *d* orbital is initially doubly occupied and lies much lower in energy than the S bonding orbital. As a consequence, only a small amount of electron density is transferred from Au to S and, in the limiting chemical form assuming an infinite energy difference, there is also no covalent contribution to the bonding. This scenario, in which Au(0) interacts with a thiyl radical, is describes as non-bonding, but strong dispersive interactions involving not only these electrons but also all electrons in the atoms remain operative. Indeed, any strong interaction between the gold and the sulfur will significantly increase the molecular polarizability and amplify the dispersion force. Another key feature is that neighbouring thiyl radicals interact with each other through superexchange interactions involving surface gold atoms as well as adatoms, removing most radical character from the net bonding.[28,62] Nevertheless, radical reactions with surface-bound sulfur can sometimes be initiated.[63]


**Figure 2.** Some standard chemical bonding scenarios.

The dominant bonding scenario found for gold compounds is Au(I)-thiolate whereas the dominant form found on metal and nanoparticle surfaces is Au(0)-thiyl. The difference between the two situations is the presence/absence of Au-Au bonds. DFT calculations indicate that the formation of Au-Au bonds involves strong interactions between *s* orbitals, the energies of which are shifted away from the Fermi energy (though the *s* band remains continuous).[4,62] Compounds described as Au(I)-thiolates are predicted to have Au-*s* dominated bonding whereas Au-*d* orbitals dominate interactions on surfaces.[45] The critical feature is that isolated gold atoms are reactive and form strong bonds to neighbouring atoms whereas gold surface atoms are noble and interact much more weakly. Indeed, just the presence of a single Au-Au bond has been described as being enough to make the chemical properties of gold dimers more similar to those of gold surfaces than to those of gold atoms.[64,65] Au-Au bonding reduces the covalent contribution to Au-S bonds but through this process the dispersive contributions to the bonding remain unaffected.[28]

**Understanding mechanisms for nanoparticle synthesis and surface protection**

Gold surfaces and nanoparticles protected by S-donor ligands are finding applications in the areas of catalysis,[66] biology and nanotechnology,[67,68] sensing and imaging,[69,70] and medical diagnostics and treatment.[71] Much effort has focussed on what products form and how they do so.[72-80] Attempts to understand all observed processes using the idea that only Au(I)-thiolates protect gold surfaces[81] have failed to rationalise the promiscuity in bonding or the

nature of reaction products, as well as the significant increase in catalytic activity when real Au(I) species are produced in, e.g., Au-O species.[37]

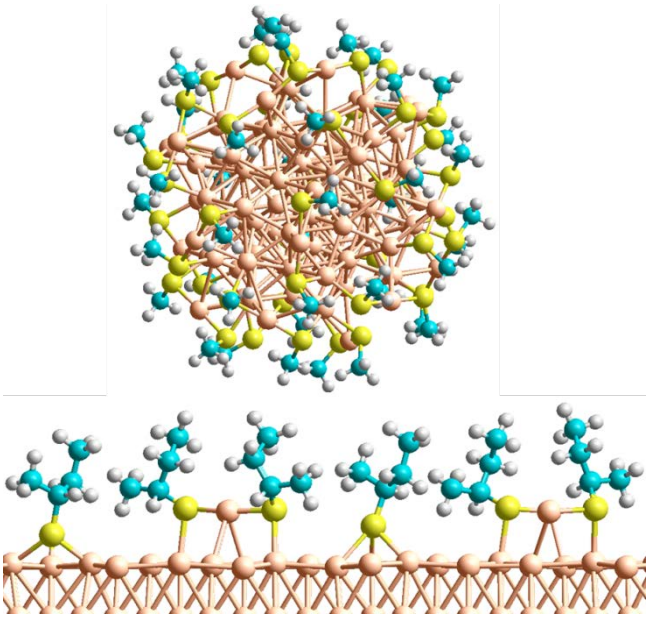

**Figure 3.** Top: $Au_{102}(SR)_{44}$ nanoparticle synthesized by Jadzinsky et al.,[82] with the actual adsorbate RSH = 4-mercaptobenzoic acid replaced with RSH = $CH_3SH$ for clarity,[62] featuring 19 RS-Au-SR units and two RS-Au-(RS)-Au-SR ones bound above an $Au_{79}$ nanoparticle core. Bottom: side view of the $(10\times\sqrt{3})-6$ phase of racemic 2-butanethiyl on Au(111),[83,84] featuring two RS-Au-SR units and two FCC-bound RS units. Brown- Au, yellow- S, cyan- C, white- H.

Observed atomic structures for monolayers above a gold nanoparticle and above a Au(111) surface are shown in Fig. 3. A critical aspect is that the adatom bonding arrangement observed in these structures has historically been drawn as[85]

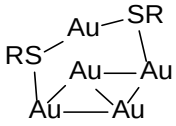


and hence described as the “staple” motif.[86] In this form the sulfur bonding is reminiscent of many Au(I)-thiolate compounds. However, as depicted in Fig. 3, there are also two more (possibly long or flexible) bonds in this system linking the gold adatom bridging the two sulfurs to the underlying surface or nanoparticle core.

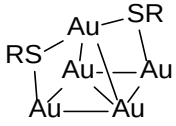

Instead, such bonding is typical of an Au(0)-thiyl species.[28] This arrangement, as well as motifs like that also shown in Fig. 3 in which SR is bound directly to face-centred cubic surface sites,

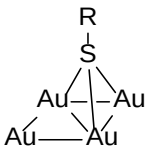


are both found on sulfur-protected Au(111) surfaces, with the scenario for each adsorbate determined by a range of factors.[84,87] Both motifs can even be observed side by side in the same self-assembled monolayer, as shown in the lower image in Fig. 3.[83,84] Directly bound motifs have also been observed on Au(100).[88] The adatom-bound motif dominates nanoparticle stabilization owing to the relaxation in strain of the Au-$Au_{adatom}$-Au bond angle afforded by nanoparticle curvature.[62] The existence of such structural diversity can only be interpreted in terms of Au(0)-thiyl bonding.

A holistic interpretation of the mechanism associated with the formation of sulfur-protected Au(111) surfaces and nanoparticles requires the understanding that different reaction pathways occur on Au(0)-thiyl surfaces compared to Au(I)-thiolate surfaces[28] (Scheme 1). Under electrochemically oxidizing conditions, gold electrodes can release Au(I) ions that can react in solution with thiolate anions $RS^-$ to form Au(I)-thiolate thin films that then cover the gold electrode.[89] The final chemical species formed protects the surface from subsequent chemical attack, but during its production the surface is first etched. These Au(I)-thiolate species are thus not really protectants at all as their formation is associated with surface destruction. On the other hand, the binding of thiols or disulfides to surfaces subsequent to initial physisorption[90,91] does not involve Au(I)-thiolate production, but results instead in surfaces protected by Au(0)-thiyl species. Chemical reaction conditions that access Au(I)-thiolate potential-energy surfaces lead to products that are fundamentally different in structure and properties to those that proceed only along Au(0)-thiyl pathways.[28]

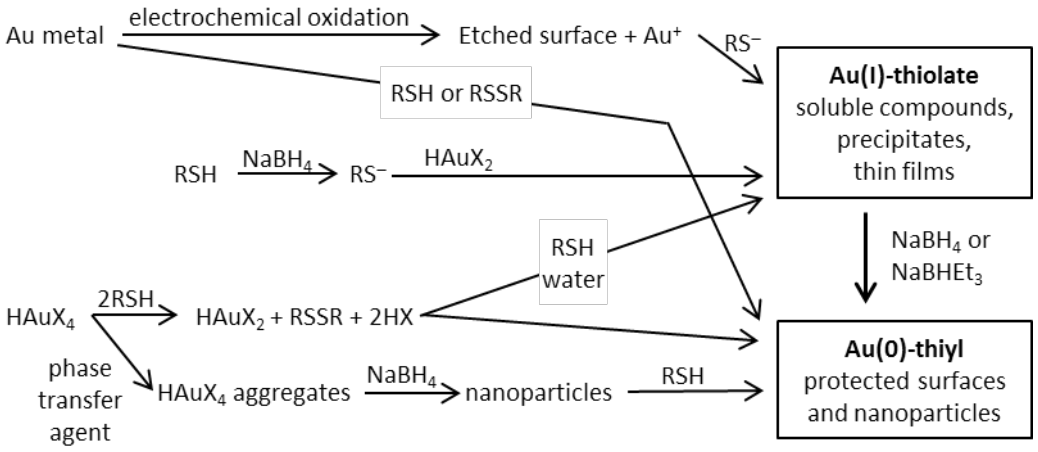


**Scheme 1:** Pathways to Au(0)-thiyl stabilized gold surfaces and nanoparticles, and pathways to Au(I)-thiolate covered etched surfaces, compounds and films.

The chemistry at play on a 2D surface is similar to that in nanoparticle synthesis, providing a basis for understanding the complexity of observed reaction products and conditions as summarized in Scheme 1. The reactions are divided into two types: those that explicitly involve thiolate anions and hence lead to Au(I)-thiolate intermediates, and those that produce protected nanoparticles directly. The one-phase Brust-Schiffrin synthesis, in which a strong reductant like sodium borohydride is mixed with a thiol,[92] results in the immediate conversion of the thiol to the thiolate, $2RSH + 2e^- \rightarrow 2RS^- + H_2$.[28] This process may involve complexation of $RS^-$ with $BH_3$[93] in a thiolate-storage mechanism[94,95] and appears to occur even in reactive solvents like methanol.[96] Under the conditions in which thiolate forms, molecular Au(I)-thiolates are also produced, these requiring subsequent reduction to give the desired nanoparticles.[33] In alternate aqueous syntheses,[97,98] nanoparticles can be formed in the absence of a strong reductant,[97] but little is known about this mechanism. Au(I)-thiolate species can be produced not only when thiolate is formed as the product of either chemical or electrochemical reduction reactions, but also when acid-base reactions can be initiated by available water.[98-104] In the two-phase Brust-Schiffrin synthesis,[29] initial reduction of $HAuCl_4$ by a thiol leads not to Au(I)-thiolates but instead to $HAuCl_2$.[99,100,105] Nanoparticles can form without any thiol involvement, with the latter molecules simply added as stabilizers after the fact,[106] somewhat akin to how thiols react with Au(111) surfaces. Analogous reactions to the Brust-Schiffrin syntheses using Se and Te start not with RSeH or RTeH, but instead with RSeSeR and RTeTeR. The diselenides and ditellerides are first oxidized to Se(II) and Te(II) species rather than being reduced to $RSe^-$ or $RTe^-$.[60,107]

A similar story thus emerges for both gold surfaces and nanoparticles covered with RS compounds: if these compounds are thiolates then thin molecular films typically precipitate over objects of interest, producing what could be described as “thiolated” surfaces. Importantly, this thiolating of a gold surface first involves surface etching. These chemical species differ in composition from those on protected gold metal and nanoparticle surfaces often mistakenly called “thiolated” surfaces. Au(0)-thiyl species actually stabilize gold surfaces and nanoparticles.[28] All of this arises through competition between strong van der Waals dispersion forces and traditional chemical bonding motifs.

**Quantifying covalent, ionic and dispersive contributions to Au-S bonds**

The picture that emerges of Au-S bonding is that in general it is made up of significant covalent, ionic and dispersion contributions. Simple analyses[28] of DFT-computed binding energies[28,62,87] obtained using the PW91 functional,[108] encompassing a wide range of bonding scenarios based on Hückel models for independent Au *s* and *d* interactions, can be applied to quantify these effects.[28] Such calculations indicate that the van der Waals interaction is on the order of 23 kcal $mol^{-1}$ (1 eV) per Au-S bond regardless of its nature, whilst the ionic and covalent terms can be 50% larger in Au(I)-thiolate compounds but can also be switched off by the introduction of Au-Au *s*-*s* interactions. The net binding energy on surfaces is typically about 30 kcal $mol^{-1}$ (1.3 eV), of which 7 kcal $mol^{-1}$ (0.3 eV) is attributed to ionic and covalent effects.[28] For disulfides, a typical surface binding energy is 8 kcal $mol^{-1}$ (0.35 eV)

per sulfur, consistent with the change in dispersion and exchange repulsion forces accompanying the change in Au-S distance from ~2.4 Å to ~3.0 Å and the 6$^{th}$ inverse-power-law scaling of the London contribution to the dispersion term.[28] A simple concept therefore allows a range of chemical properties to be rationalized. The approach is also extendable, at least qualitatively, to understand gold surfaces binding ligands other than through sulfur linkages, including those that bind through oxygen, selenium, and tellurium. Similar principles also apply to surface adducts of nitrogen and phosphorous bases as well carbon donors.[28] Of importance is how the relative strengths of the covalent and dispersive contributions change upon substitution.

**Appropriate modern computational methods**

Determining appropriate computational methods for dispersion-dominated interface modelling is currently a very active research field.[20,109] Although the first level of approximation within the DFT framework — the local density approximation (LDA) — does not account explicitly for the dispersion force and poorly represents covalent bonding, it still remains in use.[110] Improved approaches start with the generalized-gradient approximation (GGA), and an example of this, the PW91 functional,[108] It and the PBE[111] functional have been the most widely applied DFT functionals in surface chemistry, but in principle these methods also do not include the dispersion force. Given that electron correlation generated the dispersion force and seamlessly also contributes to covalent bonding, DFT functionals can misrepresent covalent bonding in a way that actually mimics dispersion at short distances.[20] Indeed, it was once claimed that PW91 was the only GGA density functional to actually include dispersion, but we showed this to be incorrect as the method has asymptotic properties typical of only covalent bonding.[112] However, both PW91 and PBE predict realistic values for the (large) physisorption energies of thiols and disulfides on gold surfaces,[28,113] and it was expected rather naively that these methods would also do well for bonds between surfaces and chemisorbed species. Their application has historically been met with success, but they do not give the “right answer for the right reason”. Failure of the approach is immediately clear when sulfur-containing ligands are replaced by harder binders like azine bases. Covalent bonding character becomes greatly reduced, as is the ability of GGAs to differentiate between covalency and dispersion, making predicted binding strengths erroneous by an order of magnitude. Also, bidentate ligands link 1,10-phenanthroline can bind very strongly to Au(0) via the dispersion force, and GGAs fail to recognize this.[114] Without explicit inclusion of dispersion, GGA functionals confuse the effects of basic chemical variations on bonding.[28]

Box 4 | **Modern computational methods combining chemical and van der Waals forces**

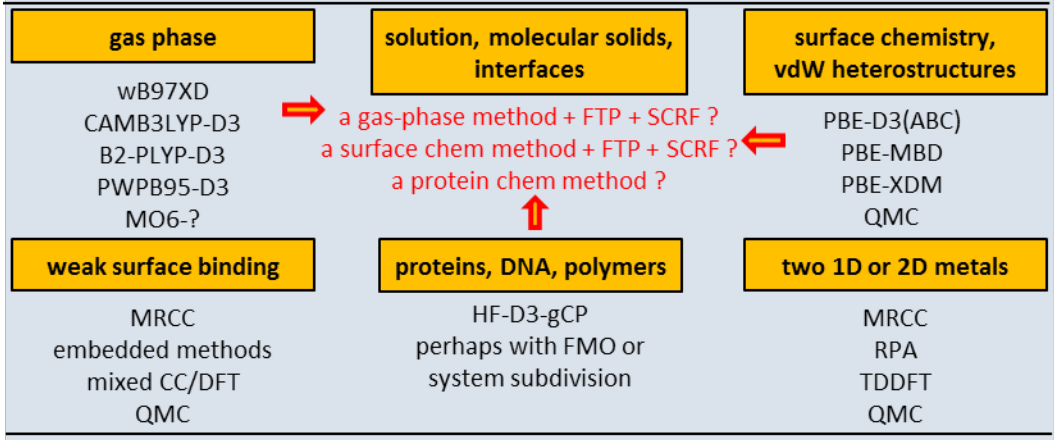


*Ab initio schemes*

- QMC- quantum Monte Carlo,[115-119] computer time $\propto 1/accuracy^2$
- MRCC- multi-reference coupled cluster[120,121]
- RPA- random phase approximation[1]

*First principles DFT schemes*

- TDDFT- time dependent density-functional theory (RPA-like)[122,123]

*Traditional ground-state DFT with dispersion corrections*

- double hybrid density functionals:[124,125] B2-PLYP,[126] PWPB95[127]
- hybrid density functional: wB97XD,[128] CAM-B3LYP,[129,130] MO6-2X[131]
- GGA density functionals: PBE[111]
- dispersion corrections to apply: D3,[132] D3(ABC),[133] MBD,[134,135] XDM,[136] VV10[137] **not** vdw-DF[138] or vdw-DF2[139]

*Speedup schemes*

- enhanced computational methods like $n^4 \log n$ scaling TDDFT, RPA[140,141]
- embedded cluster methods[142-146]
- mixed DFT with *ab initio* methods[147]
- linear scaling coupled cluster[148]
- gCP- empirical counterpoise correction,[149] works well with Hartree-Fock and D3[150]
- FMO- linear scaling scheme,[151] applies to any computational method
- system subdivision- protein linear scaling, any protein size and method combination[152]

*Empirical continuum models for solvent*

- SCRF- self-consistent reaction field for electrostatic interactions[153]
- FTP- Floris, Tomasi, and Pascual-Ahuir[154] scheme for dispersion

Beyond the GGA level, modern computational methods[1,20,109,111,115-161] (Box 4) offer better prospects for studying strong van der Waals forces and their interplay with covalent effects. To be confident in an outcome for any particular situation, a holistic understanding of the dispersion interaction and its manifold possible natures is required. All computational approaches may be categorized[1] into how thoroughly they include dispersion in a wide variety of chemical environments, allowing efficient and sufficiently accurate approaches to be identified.[20,124,157] Some basic entry-level options are categorized in Box 4, suitable for six types of applications. Two of these applications, weak surface bonding and very strong interactions between two 1D or 2D metals, are not directly relevant to the issues of this review as, in neither situation, do van der Waals forces compete with chemical forces.

However, it is comforting to know that such scenarios can be dealt with. For gas-phase problems, surface chemistry including van der Waals heterostructures, and soft matter like proteins and polymers, many application-specific methods have been recently developed that work well. However, applications like molecular solids, solution reactions and processes at interfaces between different substances are not always so clear-cut to describe, with all of the other developed methods possibly being relevant.

In terms of modern practical methods to take on nanotechnology applications in which dispersion forces compete with chemical bonding, GGA density functionals are very promising when combined with dispersion methods like D3[132] (especially in its three-body corrected form D3(ABC)[133]), the many-body dispersion method (MBD),[134,135] the Vydrov and van Voohris (VV10) method,[137] or the exchange-hole dipole model (XDM).[136] These approaches have also been shown to be successful for many other problems in surface chemistry,[20] including noncovalent binding involving graphene and van der Waals heterostructures.[159-161] Personally, we have applied the D3 correction to Au-S bonds using PW91 and obtained satisfactory results,[83,84] but we recommend combination with PBE instead as this method allows for a much cleaner separation of dispersion and covalent effects.[156] This approach has been shown to reproduce a wide range of properties for sulfur monolayers bound to Au(111) at FCC sites.[158] For situations in which a system of interest interacts with its surroundings, we have also found useful methods that treat the environmental dispersion interaction using dielectric continuum models. In this case, it is critical to verify that such implicit treatment of dispersion match well to the explicit treatment used for the represented atoms. We have found[155,156] that the implicit dispersion model of Floris, Tomasi, and Pascual Ahuir[154] (FTP) is well balanced with both the D3[132,133] and MBD[134,135] explicit dispersion treatments.

## Conclusions

The idea that only covalent and ionic forces can manifest strong bonding interactions apparent between individual atoms is questioned, as many examples of strong "soft-soft" interactions are now being identified as having large contributions from van der Waals dispersion forces. The focus of this Review has been on situations where covalent/ionic bonding favours one chemical form of a species whilst their absence favours another, leading to complex effects. Particularly considered is the interplay of ionic/covalent forces with dispersion forces in controlling the structure, reactivity, and spectroscopy of sulfur-protected gold surfaces and nanoparticles. The widely believed notion that gold surfaces are protected by Au(I)-thiolate species is dispelled, it being shown instead that conditions favouring Au(I)-thiolate production lead to very different outcomes in terms of chemical composition and system properties. The actual protecting species is Au(0)-thiyl. It is understood how for a long time it has been possible to qualitatively describe Au(I)-thiolate molecular compounds without considering the dispersion contribution, because in these species it is only a minor contributor (ca. 30%) to the bond strength. However, covalent forces can be switched off by forming Au-Au bonds to give the gold noble character, allowing the more consistent dispersive contribution to become dominant. Most likely, many more examples of

covalent/ionic and dispersion forces favouring competitive chemical structures will be discovered for situations involving soft-soft interactions. Care must be taken in computational studies where strong dispersive forces are involved, as these interactions can often be confused with covalent forces by computational methods, such that the prediction of some properties is reasonably good, but others are very poor. Appropriate computational methods must always give the right answer for the right reason, being appropriately applied.

**Acknowledgments**

Financial support from the Australian Research Council Discovery Projects grant DP160101301 and computational support from National Computational Infrastructure (d63 and no2) and INTERSECT (r88 and sb4) are gratefully acknowledged. We also acknowledge helpful discussions with Professor Jingdong Zhang and Associate Professor Qijin Chi, Technical University of Denmark.

**References**

1 Dobson, J. F. Beyond pairwise additivity in London dispersion interactions. *Int. J. Quantum Chem.* **114**, 1157-1161 (2014).
2 Tsoi, S. *et al.* Van der Waals screening by single-layer graphene and molybdenum disulfide. *ACS Nano* **8**, 12410-12417 (2014).
3 Schmidbaur, H. & Schier, A. A briefing on aurophilicity. *Chem. Soc. Rev.* **37**, 1931-1951 (2008).
4 Pyykko, P. Theoretical chemistry of gold. *Angew. Chem. Int. Ed.* **43**, 4412-4456 (2004).
5 Power, P. London Dispersion Force Effects in Sterically Crowded Inorganic and Organometallic Molecules. *Nat. Rev. Chem.* **1**, in press (2017).
6 Guo, J. D., Liptrot, D. J., Nagase, S. & Power, P. P. The multiple bonding in heavier group 14 element alkene analogues is stabilized mainly by dispersion force effects. *Chemical Science* **6**, 6235-6244 (2015).
7 Schreiner, P. R. *et al.* Overcoming lability of extremely long alkane carbon-carbon bonds through dispersion forces. *Nature* **477**, 308-311 (2011).
8 Fokin, A. A. *et al.* Stable Alkanes Containing Very Long Carbon–Carbon Bonds. *J. Am. Chem. Soc.* **134**, 13641-13650 (2012).
9 Grimme, S. & Schreiner, P. R. Steric Crowding Can Stabilize a Labile Molecule: Solving the Hexaphenylethane Riddle. *Angewandte Chemie International Edition* **50**, 12639-12642 (2011).
10 Lyngvi, E., Sanhueza, I. A. & Schoenebeck, F. Dispersion makes the difference: Bisligated transition states found for the oxidative addition of Pd(P t Bu3)2 to Ar-OSO2R and dispersion-controlled chemoselectivity in reactions with Pd[P(i Pr)(t Bu2)]2. *Organometallics* **34**, 805-812 (2015).
11 Wagner, J. P. & Schreiner, P. R. London Dispersion Decisively Contributes to the Thermodynamic Stability of Bulky NHC-Coordinated Main Group Compounds. *Journal of Chemical Theory and Computation* **12**, 231-237 (2016).
12 Hänninen, M. M., Pal, K., Day, B. M., Pugh, T. & Layfield, R. A. A three-coordinate iron-silylene complex stabilized by ligand-ligand dispersion forces. *Dalton Trans.* **45**, 11301-11305 (2016).
13 Reimers, J. R., Watts, R. O. & Klein, M. L. Intermolecular potential functions and the properties of water. *Chem. Phys.* **64**, 95 (1982).

14 Kumar, M., Chaudhari, R. V., Subramaniam, B. & Jackson, T. A. Ligand effects on the regioselectivity of rhodium-catalyzed hydroformylation: Density functional calculations illuminate the role of long-range noncovalent interactions. *Organometallics* **33**, 4183-4191 (2014).
15 Wolters, L. P., Koekkoek, R. & Bickelhaupt, F. M. Role of Steric Attraction and Bite-Angle Flexibility in Metal-Mediated C-H Bond Activation. *ACS Catalysis* **5**, 5766-5775 (2015).
16 Schweighauser, L., Strauss, M. A., Bellotto, S. & Wegner, H. A. Attraction or Repulsion? London Dispersion Forces Control Azobenzene Switches. *Angewandte Chemie - International Edition* **54**, 13436-13439 (2015).
17 Wagner, C. L. *et al.* Dispersion-Force-Assisted Disproportionation: A Stable Two-Coordinate Copper(II) Complex. *Angewandte Chemie - International Edition* **55**, 10444-10447 (2016).
18 Lomas, J. R., Baddeley, C. J., Tikhov, M. S. & Lambert, R. M. Ethyne cyclization to benzene over Cu(110). *Langmuir* **11**, 3048-3053 (1995).
19 Bilic, A., Reimers, J. R., Hush, N. S., Hoft, R. C. & Ford, M. J. Adsorption of Benzene on Copper, Silver, and Gold Surfaces. *J. Chem. Theor. Comput.* **2**, 1093-1105 (2006).
20 Reimers, J. R., Li, M., Wan, D., Gould, T. & Ford, M. J. in *Noncovalent interactions in quantum chemistry and physics: Theory and applications* Alberto Otero de la Roza & Gino DiLabio (eds.) in press (Elsevier, Amsterdam, 2017).
21 Das, P. K., Samanta, S., McQuarters, A. B., Lehnert, N. & Dey, A. Valence tautomerism in synthetic models of cytochrome P450. *Proc. Natl. Acad. Sci. U.S.A.* **113**, 6611-6616 (2016).
22 Hersleth, H.-P., Ryde, U., Rydberg, P., Görbitz, C. H. & Andersson, K. K. Structures of the high-valent metal-ion haem–oxygen intermediates in peroxidases, oxygenases and catalases. *J. Inorg. Biochem.* **100**, 460-476 (2006).
23 Reimers, J. R., McKemmish, L., McKenzie, R. H. & Hush, N. S. Bond angle variations in XH3 [X=N,P,As,Sb,Bi]: the critical role of Rydberg orbitals exposed using a diabatic state model. *Phys. Chem. Chem. Phys.* **17**, 24618-24640 (2015).
24 Reimers, J. R., McKemmish, L., McKenzie, R. H. & Hush, N. S. A unified diabatic description for electron transfer reactions, isomerization reactions, proton transfer reactions, and aromaticity. *Phys. Chem. Chem. Phys.* **17**, 24598–25617 (2015).
25 McKemmish, L. K., McKenzie, R. H., Hush, N. S. & Reimers, J. R. Quantum entanglement between electronic and vibrational degrees of freedom in molecules. *J. Chem. Phys.* **135**, 244110 (2011).
26 McKemmish, L., McKenzie, R. H., Hush, N. S. & Reimers, J. R. Electron-vibration entanglement in the Born-Oppenheimer description of chemical reactions and spectroscopy. *Phys. Chem. Chem. Phys.* **17**, 24666-24682 (2015).
27 Reimers, J. R., McKemmish, L., McKenzie, R. H. & Hush, N. S. Non-adiabatic effects in thermochemistry, spectroscopy and kinetics: the general importance of all three Born-Oppenheimer breakdown corrections. *Phys. Chem. Chem. Phys.* **17**, 24640-24665 (2015).
28 Reimers, J. R., Ford, M. J., Halder, A., Ulstrup, J. & Hush, N. S. Gold surfaces and nanoparticles are protected by Au(0)-thiyl species and are destroyed when Au(I)-thiolates form. *Proc. Natl. Acad. Sci. U.S.A.* **113**, E1424-E1433 (2016).
29 Brust, M., Walker, M., Bethell, D., Schiffrin, D. J. & Whyman, R. Synthesis of thiol-derivatized gold nanoparticles in a two-phase liquid-liquid system. *J. Chem. Soc., Chem. Commun.*, 801-802 (1994).

30 Heister, K., Zharnikov, M., Grunze, M. & Johansson, L. S. O. Adsorption of Alkanethiols and Biphenylthiols on Au and Ag Substrates: A High-Resolution X-ray Photoelectron Spectroscopy Study. *J. Phys. Chem. B* **105**, 4058-4061 (2001).
31 Heister, K., Zharnikov, M., Grunze, M., Johansson, L. S. O. & Ulman, A. Characterization of X-ray Induced Damage in Alkanethiolate Monolayers by High-Resolution Photoelectron Spectroscopy. *Langmuir* **17**, 8-11 (2001).
32 Tanaka, A., Takeda, Y., Imamura, M. & Sato, S. Dynamic final-state effect on the Au $4f$ core-level photoemission of dodecanethiolate-passivated Au nanoparticles on graphite substrates. *Physical Review B* **68**, 195415 (2003).
33 Corbierre, M. K. & Lennox, R. B. Preparation of Thiol-Capped Gold Nanoparticles by Chemical Reduction of Soluble Au(I)−Thiolates. *Chem. Mater.* **17**, 5691-5696 (2005).
34 Shaporenko, A., Zharnikov, M., Feulner, P. & Menzel, D. Quantitative analysis of temperature effects in radiation damage of thiolate-based self-assembled monolayers. *J. Phys.: Condens. Matter* **18**, S1677 (2006).
35 Park, E. D. & Lee, J. S. Effects of Pretreatment Conditions on CO Oxidation over Supported Au Catalysts. *J. Catal.* **186**, 1-11 (1999).
36 Venezia, A. M. *et al.* Relationship between Structure and CO Oxidation Activity of Ceria-Supported Gold Catalysts. *J. Phys. Chem. B* **109**, 2821-2827 (2005).
37 Casaletto, M. P., Longo, A., Martorana, A., Prestianni, A. & Venezia, A. M. XPS study of supported gold catalysts: the role of Au(0) and Au(+delta) species as active sites. *Surf. Interface Anal.* **38**, 215-218 (2006).
38 Mikhlin, Y. L., Nasluzov, V. A., Romanchenko, A. S., Shor, A. M. & Pal'yanova, G. A. XPS and DFT studies of the electronic structures of AgAuS and Ag3AuS2. *J. Alloys Compd.* **617**, 314-321 (2014).
39 Liao, L. *et al.* Structure of Chiral Au44(2,4-DMBT)26 Nanocluster with an 18-Electron Shell Closure. *J. Am. Chem. Soc.* **138**, 10425-10428 (2016).
40 McNeillie, A., Brown, D. H., Smith, W. E., Gibson, M. & Watson, L. X-ray photoelectron spectra of some gold compounds. *Journal of the Chemical Society, Dalton Transactions*, 767-770 (1980).
41 Behera, M. & Ram, S. Inquiring the mechanism of formation, encapsulation, and stabilization of gold nanoparticles by poly(vinyl pyrrolidone) molecules in 1-butanol. *Appl. Nanosci.* **4**, 247-254 (2014).
42 Senthilnathan, J., Rao, K. S., Lin, W.-H., Ting, J.-M. & Yoshimura, M. Formation of reusable Au-acetonitrile polymers and N-doped graphene catalyst under UV light via submerged liquid plasma process. *J. Mater. Chem. A* **3**, 3035-3043 (2015).
43 Zhang, P. & Sham, T. K. X-Ray Studies of the Structure and Electronic Behavior of Alkanethiolate-Capped Gold Nanoparticles: The Interplay of Size and Surface Effects. *Phys. Rev. Lett.* **90**, 245502 (2003).
44 de la Llave, E., Clarenc, R., Schiffrin, D. J. & Williams, F. J. Organization of Alkane Amines on a Gold Surface: Structure, Surface Dipole, and Electron Transfer. *J. Phys. Chem. C* **118**, 468-475 (2014).
45 Chaudhuri, A. *et al.* The structure of the Au(111)/methylthiolate interface. New insights from near-edge x-ray absorption spectroscopy and x-ray standing waves. *J. Chem. Phys.* **130**, 124708 (2009).
46 Mikhlin, Y. *et al.* XAS and XPS examination of the Au–S nanostructures produced via the reduction of aqueous gold(III) by sulfide ions. *J. Electron Spectrosc. Relat. Phenom.* **177**, 24-29 (2010).
47 Corthey, G. *et al.* Synthesis and Characterization of Gold@Gold(I)−Thiomalate Core@Shell Nanoparticles. *ACS Nano* **4**, 3413-3421 (2010).

48 Simms, G. A., Padmos, J. D. & Zhang, P. Structural and electronic properties of protein/thiolate-protected gold nanocluster with "staple" motif: A XAS, L-DOS, and XPS study. *J. Chem. Phys.* **131**, 214703/214701-214703/214709 (2009).
49 Pearson, R. G. Hard and soft acids and bases HSAB.1. Fundamental principles. *J. Chem. Educ.* **45**, 581-587 (1968).
50 Pearson, R. G. Hard and soft acids and bases - the evolution of a chemical concept. *Coord. Chem. Rev.* **100**, 403-425 (1990).
51 Ayers, P. W., Parr, R. G. & Pearson, R. G. Elucidating the hard/soft acid/base principle: A perspective based on half-reactions. *J. Chem. Phys.* **124**, 194107 (2006).
52 Selinger, B. *Chemistry in the Marketplace*. (Allen & Unwin, Sydney, 1999).
53 Barton, E. J. *et al.* ExoMol molecular line lists V: the ro-vibrational spectra of NaCl and KCl. *Mon. Not. R. Astron. Soc.* **442**, 1821-1829 (2014).
54 Reckien, W., Eggers, M. & Bredow, T. Theoretical study of the adsorption of benzene on coinage metals. *Beilstein J. Org. Chem.* **10**, 1775-1784 (2014).
55 Liu, W. *et al.* Quantitative Prediction of Molecular Adsorption: Structure and Binding of Benzene on Coinage Metals. *Phys. Rev. Lett.* **115**, 036104 (2015).
56 Hohman, J. N. *et al.* Exchange Reactions between Alkanethiolates and Alkaneselenols on Au{111}. *J. Am. Chem. Soc.* **136**, 8110-8121 (2014).
57 Schmøkel, M. S. *et al.* Testing the Concept of Hypervalency: Charge Density Analysis of K2SO4. *Inorg. Chem.* **51**, 8607-8616 (2012).
58 Tang, Q. & Jiang, D.-E. Insights into the PhC≡C/Au Interface. *J. Phys. Chem. C* **119**, 10804-10810 (2014).
59 Zaba, T. *et al.* Formation of Highly Ordered Self-Assembled Monolayers of Alkynes on Au(111) Substrate. *J. Am. Chem. Soc.* **136**, 11918-11921 (2014).
60 Li, Y., Silverton, L. C., Haasch, R. & Tong, Y. Y. Alkanetelluroxide-Protected Gold Nanoparticles. *Langmuir* **24**, 7048-7053 (2008).
61 Kurashige, W. *et al.* Au25 Clusters Containing Unoxidized Tellurolates in the Ligand Shell. *J. Phys. Chem. Lett.* **5**, 2072-2076 (2014).
62 Reimers, J. R., Wang, Y., Cankurtaran, B. O. & Ford, M. J. Chemical Analysis of the Superatom Model for Sulfur-Stabilized Gold Nanoparticles. *J. Am. Chem. Soc.* **132**, 8378-8384 (2010).
63 Zhang, J. & Ulstrup, J. Oxygen-free in situ scanning tunnelling microscopy. *J. Electroanal. Chem.* **599**, 213-220 (2007).
64 McAdon, M. H. & Goddard, W. A. Charge density waves, spin density waves, and Peierls distortions in one‐dimensional metals. I. Hartree‐Fock studies of Cu, Ag, Au, Li, and Na. *J. Chem. Phys.* **88**, 277-302 (1988).
65 McAdon, M. H. & Goddard, W. A. Charge density waves, spin density waves, and Peierls distortions in one-dimensional metals. 2. Generalized valence bond studies of copper, silver, gold, lithium and sodium. *J. Phys. Chem.* **92**, 1352-1365 (1988).
66 Fang, J. *et al.* Recent advances in the synthesis and catalytic applications of ligand-protected, atomically precise metal nanoclusters. *Coord. Chem. Rev.* **322**, 1-29 (2016).
67 De, M., Ghosh, P. S. & Rotello, V. M. Applications of Nanoparticles in Biology. *Advanced Materials* **20**, 4225-4241 (2008).
68 Sapsford, K. E. *et al.* Functionalizing Nanoparticles with Biological Molecules: Developing Chemistries that Facilitate Nanotechnology. *Chem. Rev.* **113**, 1904-2074 (2013).
69 Saha, K., Agasti, S. S., Kim, C., Li, X. & Rotello, V. M. Gold Nanoparticles in Chemical and Biological Sensing. *Chem. Rev.* **112**, 2739-2779 (2012).
70 Zhang, L. & Wang, E. Metal nanoclusters: New fluorescent probes for sensors and bioimaging. *Nano Today* **9**, 132-157 (2014).

71 Muthu, M. S., Agrawal, P. & Singh, S. Theranostic nanomedicine of gold nanoclusters: an emerging platform for cancer diagnosis and therapy. *Nanomedicine* **11**, 327-330 (2016).
72 Whitesides, G. M. & Laibinis, P. E. Wet chemical approaches to the characterization of organic surfaces: self-assembled monolayers, wetting, and the physical-organic chemistry of the solid-liquid interface. *Langmuir* **6**, 87-96 (1990).
73 Schmidbaur, H. Ludwig Mond Lecture. High-carat gold compounds. *Chem. Soc. Rev.* **24**, 391-400 (1995).
74 Love, J. C., Estroff, L. A., Kriebel, J. K., Nuzzo, R. G. & Whitesides, G. M. Self-Assembled Monolayers of Thiolates on Metals as a Form of Nanotechnology. *Chem. Rev.* **105**, 1103-1169 (2005).
75 Hutchings, G. J., Brust, M. & Schmidbaur, H. Gold - an introductory perspective. *Chem. Soc. Rev.* **37**, 1759-1765 (2008).
76 Skrabalak, S. E. *et al.* Gold Nanocages: Synthesis, Properties, and Applications. *Acc. Chem. Res.* **41**, 1587-1595 (2008).
77 Sardar, R., Funston, A. M., Mulvaney, P. & Murray, R. W. Gold Nanoparticles: Past, Present, and Future. *Langmuir* **25**, 13840-13851 (2009).
78 Zhao, P., Li, N. & Astruc, D. State of the art in gold nanoparticle synthesis. *Coord. Chem. Rev.* **257**, 638-665 (2013).
79 Kurashige, W., Niihori, Y., Sharma, S. & Negishi, Y. Precise synthesis, functionalization and application of thiolate-protected gold clusters. *Coord. Chem. Rev.* **320–321**, 238-250 (2016).
80 Goswami, N., Yao, Q., Chen, T. & Xie, J. Mechanistic Exploration and Controlled Synthesis of Precise Thiolate-Gold Nanoclusters. *Coord. Chem. Rev.* **in press** (2016).
81 Pensa, E. *et al.* The Chemistry of the Sulfur–Gold Interface: In Search of a Unified Model. *Acc. Chem. Res.* **45**, 1183-1192 (2012).
82 Jadzinsky, P. D., Calero, G., Ackerson, C. J., Bushnell, D. A. & Kornberg, R. D. Structure of a thiol monolayer-protected gold nanoparticle at 1.1 angstrom resolution. *Science* **318**, 430-433 (2007).
83 Ouyang, R. *et al.* Intermixed adatom and surface bound adsorbates in regular self-assembled monolayers of racemic 2-butanethiol on Au(111) *ChemPhysChem* **16**, 928–932 (2015).
84 Yan, J. *et al.* Controlling the stereochemistry and regularity of butanethiol self-assembled monolayers on Au(111) *J. Amer. Chem. Soc.* **136**, 17087–17094 (2014).
85 Maksymovych, P., Sorescu, D. C. & Yates, J. T., Jr. Gold-adatom-mediated bonding in self-assembled short-chain alkanethiolate species on the Au(111) surface. *Phys. Rev. Lett.* **97**, 146103 (2006).
86 Jiang, D.-E., Tiago, M. L., Luo, W. D. & Dai, S. The "Staple" motif: A key to stability of thiolate-protected gold nanoclusters. *J. Am. Chem. Soc.* **130**, 2777 (2008).
87 Wang, Y. *et al.* Chain-Branching Control of the Atomic Structure of Alkanethiol-Based Gold-Sulfur Interfaces. *J. Am. Chem. Soc.* **133**, 14856-14859 (2011).
88 Grumelli, D., Maza, F. L., Kern, K., Salvarezza, R. C. & Carro, P. Surface Structure and Chemistry of Alkanethiols on Au(100)-(1 × 1) Substrates. *J. Phys. Chem. C* **120**, 291-296 (2016).
89 Chadha, R. K., Kumar, R. & Tuck, D. G. The direct electrochemical synthesis of thiolato complexes of copper, silver, and gold; the molecular structure of [Cu(SC6H4CH3-o)(1,10-phenanthroline)]2.CH3CN. *Can. J. Chem.* **65**, 1336-1342 (1987).
90 Wang, Y., Hush, N. S. & Reimers, J. R. Understanding the Chemisorption of 2-Methyl-2-propanethiol on Au(111). *J. Phys. Chem. C* **111**, 10878-10885 (2007).

91 Bandyopadhyay, S., Chattopadhyay, S. & Dey, A. The protonation state of thiols in self-assembled monolayers on roughened Ag/Au surfaces and nanoparticles. *Phys. Chem. Chem. Phys.* **17**, 24866-24873 (2015).
92 Brust, M., Fink, J., Bethell, D., Schiffrin, D. J. & Kiely, C. Synthesis and reactions of functionalized gold nanoparticles. *J. Chem. Soc., Chem. Commun.*, 1655-1656 (1995).
93 Romero, E. A., Peltier, J. L., Jazzar, R. & Bertrand, G. Catalyst-free dehydrocoupling of amines, alcohols, and thiols with pinacol borane and 9-borabicyclononane (9-BBN). *Chem. Commun.* **52**, 10563-10565 (2016).
94 Civit, M. G. *et al.* Ynones Merge Activation/Conjugate Addition of Chalcogenoborates ArE-Bpin (E=Se, S). *Adv. Synth. Catal.* **357**, 3098-3103 (2015).
95 Solé, C. & Fernández, E. Alkoxide Activation of Aminoboranes towards Selective Amination. *Angew. Chem. Int. Ed.* **52**, 11351-11355 (2013).
96 Davis, R. E. & Gottbrath, J. A. Boron Hydrides. V. Methanolysis of Sodium Borohydride. *J. Am. Chem. Soc.* **84**, 895-898 (1962).
97 Negishi, Y. & Tsukuda, T. One-Pot Preparation of Subnanometer-Sized Gold Clusters via Reduction and Stabilization by meso-2,3-Dimercaptosuccinic Acid. *J. Am. Chem. Soc.* **125**, 4046-4047 (2003).
98 Schaaff, T. G., Knight, G., Shafigullin, M. N., Borkman, R. F. & Whetten, R. L. Isolation and Selected Properties of a 10.4 kDa Gold:Glutathione Cluster Compound. *J. Phys. Chem. B* **102**, 10643-10646 (1998).
99 Goulet, P. J. G. & Lennox, R. B. New Insights into Brust−Schiffrin Metal Nanoparticle Synthesis. *J. Am. Chem. Soc.* **132**, 9582-9584 (2010).
100 Li, Y., Zaluzhna, O. & Tong, Y. J. Critical Role of Water and the Structure of Inverse Micelles in the Brust–Schiffrin Synthesis of Metal Nanoparticles. *Langmuir* **27**, 7366-7370 (2011).
101 Perala, S. R. K. & Kumar, S. On the Mechanism of Metal Nanoparticle Synthesis in the Brust–Schiffrin Method. *Langmuir* **29**, 9863-9873 (2013).
102 Yu, C. *et al.* Investigation on the Mechanism of the Synthesis of Gold(I) Thiolate Complexes by NMR. *J. Phys. Chem. C* **118**, 10434-10440 (2014).
103 Uehara, A. *et al.* Electrochemical Insight into the Brust–Schiffrin Synthesis of Au Nanoparticles. *J. Am. Chem. Soc.* **137**, 15135-15144 (2015).
104 Marbella, L. E. *et al.* Description and Role of Bimetallic Prenucleation Species in the Formation of Small Nanoparticle Alloys. *J. Am. Chem. Soc.* **137**, 15852-15858 (2015).
105 Zhu, L. *et al.* New Insight into Intermediate Precursors of Brust–Schiffrin Gold Nanoparticles Synthesis. *J. Phys. Chem. C* **117**, 11399-11404 (2013).
106 Graham, T. R., Renslow, R., Govind, N. & Saunders, S. R. Precursor Ion–Ion Aggregation in the Brust–Schiffrin Synthesis of Alkanethiol Nanoparticles. *J. Phys. Chem. C* **120**, 19837-19847 (2016).
107 Zaluzhna, O., Li, Y., Zangmeister, C., Allison, T. C. & Tong, Y. J. Mechanistic insights on one-phase vs. two-phase Brust-Schiffrin method synthesis of Au nanoparticles with dioctyl-diselenides. *Chemical Communications* **48**, 362-364 (2012).
108 Perdew, J. P. & Wang, Y. Accurate and simple analytic representation of the electron-gas correlation energy. *Phys. Rev. B* **45**, 13244-13249 (1992).
109 Otero de la Roza, A. & DiLabio, G. (eds). *Noncovalent interactions in quantum chemistry and physics: Theory and applications*. (Elsevier, Amsterdam, 2017).
110 Mäkinen, V., Koskinen, P. & Häkkinen, H. Modeling thiolate-protected gold clusters with density-functional tight-binding. *The European Physical Journal D* **67**, 38 (2013).
111 Perdew, J. P., Burke, W. & Ernzerhof, M. Generalized gradient approximation made simple. *Phys. Rev. Lett.* **77**, 3865-3868 (1996).

112 Bilic, A., Reimers, J. R., Hush, N. S. & Hafner, J. Adsorption of ammonia on the gold (111) surface. *J. Chem. Phys.* **116**, 8981-8987 (2002).
113 Wang, Y., Hush, N. S. & Reimers, J. R. Formation of Gold-Methanethiyl Self-Assembled Monolayers. *J. Am. Chem. Soc.* **129**, 14532-14533 (2007).
114 Cafe, P. F. *et al.* Chemisorbed and Physisorbed Structures for 1,10-Phenanthroline and Dipyrido[3,2-a:2',3'-c]phenazine on Au(111). *J. Phys. Chem. C* **111**, 17285-17296 (2007).
115 Towler, M. D. in *Computational Methods for Large Systems: Electronic Structure Approaches for Biotechnology and Nanotechnology* J. R. Reimers (eds.) 119-166 (Wiley, Hoboken NJ, 2011).
116 Al-Hamdani, Y. S., Ma, M., Alfè, D., von Lilienfeld, O. A. & Michaelides, A. Communication: Water on hexagonal boron nitride from diffusion Monte Carlo. *J. Chem. Phys.* **142**, 181101 (2015).
117 Booth, G. H., Grüneis, A., Kresse, G. & Alavi, A. Towards an exact description of electronic wavefunctions in real solids. *Nature* **493**, 365-370 (2013).
118 Booth, G. H., Thom, A. J. W. & Alavi, A. Fermion Monte Carlo without fixed nodes: A game of life, death, and annihilation in Slater determinant space. *J. Chem. Phys.* **131**, 054106 (2009).
119 Dubecký, M., Mitas, L. & Jurečka, P. Noncovalent Interactions by Quantum Monte Carlo. *Chem. Rev.* **116**, 5188-5215 (2016).
120 Grüneis, A. A coupled cluster and Møller-Plesset perturbation theory study of the pressure induced phase transition in the LiH crystal. *J. Chem. Phys.* **143**, 102817 (2015).
121 Voloshina, E. & Paulus, B. First Multireference Correlation Treatment of Bulk Metals. *J. Chem. Theory Comput.* **10**, 1698-1706 (2014).
122 Olsen, T. & Thygesen, K. S. *Phys. Rev. B* **88**, 115131 (2013).
123 Gould, T. *J. Chem. Phys.* **137**, 111101 (2012).
124 Goerigk, L. & Grimme, S. Double-hybrid density functionals. *WIREs Comput. Mol. Sci.* **4**, 576-600 (2014).
125 Grimme, S., Hansen, A., Brandenburg, J. G. & Bannwarth, C. Dispersion-Corrected Mean-Field Electronic Structure Methods. *Chem. Rev.* **116**, 5105-5154 (2016).
126 Grimme, S. Semiempirical hybrid density functional with perturbative second-order correlation. *J. Chem. Phys.* **124**, 034108 (2006).
127 Goerigk, L. & Grimme, S. Efficient and Accurate Double-Hybrid-Meta-GGA Density Functionals—Evaluation with the Extended GMTKN30 Database for General Main Group Thermochemistry, Kinetics, and Noncovalent Interactions. *Journal of Chemical Theory and Computation* **7**, 291-309 (2011).
128 Chai, J.-D. & Head-Gordon, M. Long-range corrected hybrid density functionals with damped atom-atom dispersion corrections. *Phys. Chem. Chem. Phys.* **10**, 6615-6620 (2008).
129 Yanai, T., Tew, D. P. & Handy, N. C. A new hybrid exchange-correlation functional using the Coulomb-attenuating method (CAM-B3LYP). *Chem. Phys. Lett.* **393**, 51-57 (2004).
130 Cai, Z.-L., Crossley, M. J., Reimers, J. R., Kobayashi, R. & Amos, R. D. Density-functional theory for charge-transfer: the nature of the N-bands of porphyrins and chlorophylls revealed through CAM-B3LYP, CASPT2, and SAC-CI calculations. *J. Phys. Chem. B* **110**, 15624-15632 (2006).
131 Zhao, Y. & Truhlar, D. G. The M06 suite of density functionals for main group thermochemistry, thermochemical kinetics, noncovalent interactions, excited states,

and transition elements: two new functionals and systematic testing of four M06-class functionals and 12 other functionals. *Theor. Chem. Acc.* **120**, 215-241 (2008).
132 Grimme, S., Ehrlich, S. & Goerigk, L. Effect of the damping function in dispersion corrected density functional theory. *J. Comput. Chem.* **32**, 1456-1465 (2011).
133 Grimme, S., Antony, J., Ehrlich, S. & Krieg, H. A consistent and accurate ab initio parametrization of density functional dispersion correction (DFT-D) for the 94 elements H-Pu. *J. Chem. Phys.* **132**, 154104 (2010).
134 Tkatchenko, A., Distasio, R. A., Car, R. & Scheffler, M. Accurate and efficient method for many-body van der Waals interactions. *Phys. Rev. Lett.* **108**, 236402 (2012).
135 Ambrosetti, A., Reilly, A. M., Distasio Jr, R. A. & Tkatchenko, A. Long-range correlation energy calculated from coupled atomic response functions. *J. Chem. Phys.* **140**, 18a508 (2014).
136 Christian, M. S., Otero-de-la-Roza, A. & Johnson, E. R. Surface Adsorption from the Exchange-Hole Dipole Moment Dispersion Model. *J. Chem. Theory Comput.* **12**, 3305-3315 (2016).
137 Vydrov, O. A. & Van Voorhis, T. Nonlocal van der Waals density functional: The simpler the better. *J. Chem. Phys.* **133**, 244103 (2010).
138 Dion, M., Rydberg, H., Schröder, E., Langreth, D. C. & Lundqvist, B. I. Van der Waals density functional for general geometries. *Phys. Rev. Lett.* **92**, 246401-246401 (2004).
139 Lee, K., Murray, É. D., Kong, L., Lundqvist, B. I. & Langreth, D. C. Higher-accuracy van der Waals density functional. *Phys. Rev. B* **82**, 081101 (2010).
140 Erhard, J., Bleiziffer, P. & Görling, A. Power Series Approximation for the Correlation Kernel Leading to Kohn-Sham Methods Combining Accuracy, Computational Efficiency, and General Applicability. *Phys. Rev. Lett.* **117**, 143002 (2016).
141 Eshuis, H., Bates, J. E. & Furche, F. Electron correlation methods based on the random phase approximation. *Theor. Chem. Acc.* **131**, 1084 (2012).
142 Gillan, M. J., Alfè, D., Bygrave, P. J., Taylor, C. R. & Manby, F. R. Energy benchmarks for water clusters and ice structures from an embedded many-body expansion. *J. Chem. Phys.* **139**, 114101 (2013).
143 Paulus, B. The method of increments—a wavefunction-based ab initio correlation method for solids. *Phys. Rep.* **428**, 1-52 (2006).
144 Muller, C. & Paulus, B. Wavefunction-based electron correlation methods for solids. *Phys. Chem. Chem. Phys.* **14**, 7605-7614 (2012).
145 Stoll, H., Paulus, B. & Fulde, P. An incremental coupled-cluster approach to metallic lithium. *Chem. Phys. Lett.* **469**, 90-93 (2009).
146 de Lara-Castells, M. P., Mitrushchenkov, A. O. & Stoll, H. Combining density functional and incremental post-Hartree-Fock approaches for van der Waals dominated adsorbate-surface interactions: Ag2/graphene. *J. Chem. Phys.* **143**, 102804 (2015).
147 Lara-Castells, M. P. d. *et al.* A combined periodic density functional and incremental wave-function-based approach for the dispersion-accounting time-resolved dynamics of 4He nanodroplets on surfaces: 4He/graphene. *J. Chem. Phys.* **141**, 151102 (2014).
148 Rolik, Z., Szegedy, L., Ladjánszki, I., Ladóczki, B. & Kállay, M. An efficient linear-scaling CCSD(T) method based on local natural orbitals. *J. Chem. Phys.* **139**, 094105 (2013).

149 Kruse, H. & Grimme, S. A geometrical correction for the inter- and intra-molecular basis set superposition error in Hartree-Fock and density functional theory calculations for large systems. *J. Chem. Phys.* **136**, 154101 (2012).
150 Goerigk, L. & Reimers, J. R. Efficient Methods for the Quantum Chemical Treatment of Protein Structures: The Effects of London-Dispersion and Basis-Set Incompleteness on Peptide and Water-Cluster Geometries. *J. Chem. Theory Comput.* **9**, 3240-3251 (2013).
151 Fedorov, D. G., Nagata, T. & Kitaura, K. Exploring chemistry with the fragment molecular orbital method. *Phys. Chem. Chem. Phys.* **14**, 7562-7577 (2012).
152 Canfield, P., Dahlbom, M. G., Reimers, J. R. & Hush, N. S. Density-functional geometry optimization of the 150000-atom photosystem-I trimer. *J. Chem. Phys.* **124**, 024301 (2006).
153 Tomasi, J., Mennucci, B. & Cammi, R. Quantum mechanical continuum solvation models. *Chem. Rev.* **105**, 2999-3093 (2005 ).
154 Floris, F. M., Tomasi, J. & Pascual Ahuir, J. L. Dispersion and Repulsion Contributions to the Solvation Energy: Refinements to a Simple Computational Model in the Continuum Approximation. *J. Computat. Chem.* **12**, 784-791 (1991).
155 Reimers, J. R. *et al.* From chaos to Order: Chain-Length Dependence of the Free Energy of Formation of Tetraalkylporphyrin Self-Assembled Monolayer Polymorphs *J. Phys. Chem. C* **120**, 1739-1748 (2016).
156 Reimers, J. R. *et al.* A priori calculations of the free energy of formation from solution of polymorphic self-assembled monolayers. *Proc. Natl. Acad. Sci. U.S.A.* **112**, E6101-E6110 (2015).
157 Goerigk, L. & Grimme, S. A thorough benchmark of density functional methods for general main group thermochemistry, kinetics, and noncovalent interactions. *Phys. Chem. Chem. Phys.* **13**, 6670-6688 (2011).
158 Fajín, J. L. C., Teixeira, F., Gomes, J. R. B. & Cordeiro, M. N. D. S. Effect of van der Waals interactions in the DFT description of self-assembled monolayers of thiols on gold. *Theoretical Chemistry Accounts* **134** (2015).
159 Geim, A. K. & Grigorieva, I. V. Van der Waals heterostructures. *Nature* **499**, 419-425 (2013).
160 Voloshina, E. & Dedkov, Y. S. Graphene on metallic surfaces: problems and perspectives. *Phys. Chem. Chem. Phys.* **14**, 13502 (2012).
161 Gao, W. & Tkatchenko, A. Sliding mechanisms in multilayered hexagonal boron nitride and graphene: The effects of directionality, thickness, and sliding constraints. *Phys. Rev. Lett.* **114**, 096101 (2015).